Electrification of a Milstein-type Catalyst for Alcohol Reformation

Niklas von Wolff,*[a] Damien Tocqueville,[a] Esther Nubret,[a] Marc Robert,[a,b] and David Milstein [c]

Novel energy and atom efficiency processes will be keys to develop the sustainable chemical industry of the future. Electrification could play an important role, by allowing to fine-tune energy input and using the ideal redox agent: the electron. Here we demonstrate that a commercially available Milstein ruthenium cata-lyst (1) can be used to promote the electrochemical oxidation of ethanol to ethyl acetate and acetate, thus demonstrating the four electron oxidation under preparative conditions. Cyclic voltammetry and DFT-calculations are used to devise a possible catalytic cycle based on a thermal chemical step generating the key hydride intermediate. Successful electrification of Milstein-type catalysts opens pathway to use alcohols as renewable feedstock for the generation of esters and other key building blocks in organic chemistry, thus contributing to increase energy efficiency in organic redox chemistry.

In order to achieve the goals of the Sustainable Development Scenario (SDS) of the International Energy Agency, the chemical industry's emission should decline by around 10 % before 2030.[1,2] This could be achieved by increasing energy efficiency and the usage of renewable feedstocks. In this respect, molecular electrocatalytic alcohol oxidation could be powerful tool by potentially providing energy and atom efficiency for organic synthesis and energy applications.[3,4,2,5–7] Besides the use of aminoxyl-derivatives,[8–13] especially the seminal work of Vizza, Bianchini and Grützmacher demonstrated that (transfer)-hydrogenation (TH) catalysts could be activated electrochemically and used in a so-called "organometallic fuel cell".[14] Other TH systems are however mostly limited to two electron oxidations of secondary or benzylic alcohols.[15–20] As an exception, Waymouth *et al.* recently reported an example of the intramolecular coupling of vicinal benzylic alcohols to the corresponding esters.[19,21] In order to extend the range of possible catalysts candidates, the Waymouth group recently explored the possibility to use an iron-based acceptor-less alcohol dehydrogenation (AAD) catalysts[22] for electrocatalytic alcohol oxidation.[23] The stability under electrochemical conditions in this case is limited to <2 turnovers, but it opens the door to explore a wide range of AAD reactions under electrochemical conditions. Here, we demonstrate that a commercially available Milstein-type AAD catalyst (**1**)[24] is competent for the electrocatalytic alcohol oxidation of ethanol to ethyl acetate and acetate.

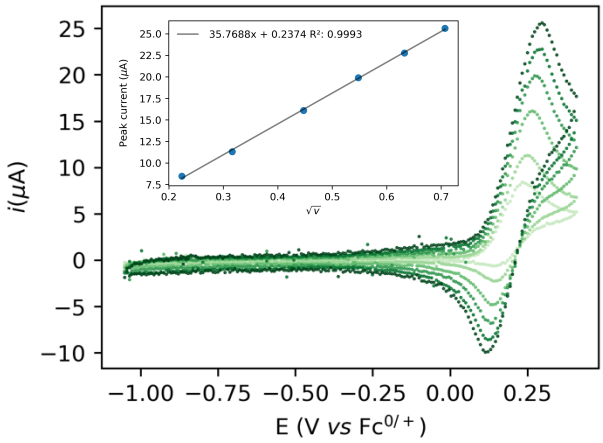

Figure 1. Scan rate dependence of a 1 mM solution of 1 in in 2:1 THF/DFB + 0.2 M NaPF6 (from light to dark green: 0.05, 0.1, 0.2, 0.3, 0.4 and 0.5 V/s, 3 mm GC electrode). Inset: evolution of the peak current as a function of the square root of the scan rate.

The cyclic voltammogram (CV) of complex **1** (Figure 1) shows a quasi-reversible diffusive one electron oxidation wave at 0.2 V (all potentials are referenced *vs* Fc^{+}/Fc^{0}) in 0.2 M $NaPF_6$ THF/DFB (2:1) (DFB = 1,2 Difluoro Benzene) as determined by DOSY-NMR spectroscopy (see SI, section 2.2). The addition of **1** to a 10 mM sodium ethoxide (NaOEt) solution in 200 mM ethanol (EtOH) in 0.1 M $NaPF_6$ (2:1 THF/DFB) gives rise to several waves at ca. -0.5, 0.0 and 0.2 V with currents significantly higher than in the absence of catalysts or substrate, indicative of possible catalytic turnover (Figure 2). Gradual increase of the EtOH concentration from 200 mM to 1 M is accompanied by the disappearance of the first wave at -0.5 V, while a new oxidation wave appears at ca. -0.25 V (Figure 2, light to dark green traces).

[a] *Laboratoire d'Electrochimie Moléculaire Université de Paris, CNRS F-75006 Paris, France.*
[b] *Institut Universitaire de France (IUF), F-75005 Paris, France.*
[c] *Department of Molecular Chemistry and Materials Science, The Weizmann Institute of Science Rehovot 7610001, Israel.*
Electronic Supplementary Information (ESI) available including experimental procedures, CV-characterization of key intermediates, CPE results, DFT-calculated redox potentials and BDFEs, See DOI: 10.1039/x0xx00000x

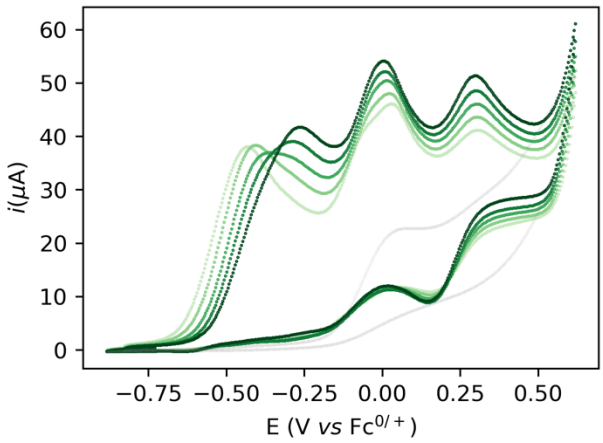

Figure 2. CVs of 10 mM NaOEt (grey) and of 5 mM **1** + 10 mM NaOEt with increasing concentrations of EtOH (from light to dark green: 200, 400, 600, 800 and 1000 mM) in 2:1 THF/DFB + 0.2 M $NaPF_6$. Scan rate 0.1 V/s, electrode: 3 mm diameter GC electrode.

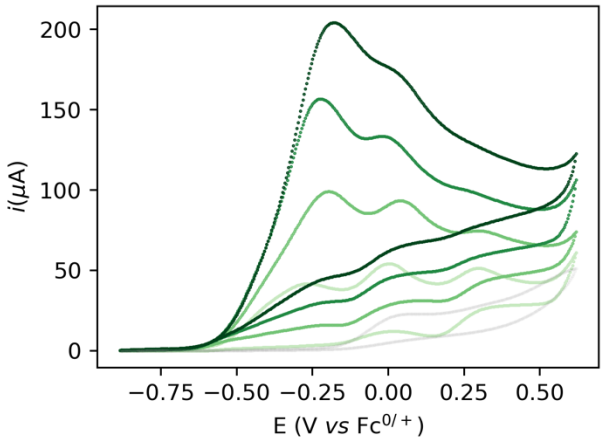

Figure 3. CV of 5 mM NaOEt (grey), 5 mM of **1** + 1M EtOH with varying concentrations of base (5, 10, 15, and 20 mM NaOEt, light to dark green) in 2:1 THF/DFB + 0.2 M $NaPF_6$. Scan rate 0.1 V/s, electrode: 3 mm diameter GC electrode.

Increasing the base loading gradually from 5 to 20 mM yields a stark increase of current at this new wave at ca. -0.25 V (Figure 3). Using $(TBA)PF_6$ instead of $NaPF_6$ (used to avoid Hofmann-elimination[25]) gave similar results (see SI, section 2.2-2.5). In order to assess catalytic turnover under preparative conditions, controlled potential electrolysis (CPE) was performed. CPE experiments were run in pure ethanol (to reduce cell resistance) in the presence of 0.1 M electrolyte of well soluble bases (e.g. NaOEt, LiOH, see SI section 4). CPE in 0.1 M LiOH with 1 mM **1** at E = 0 V vs $Fc^{0/+}$ delivered ca. 15 mM of acetate and 6 mM of ethyl acetate, corresponding to 21 turnovers (per 4 electrons, or 42 turnovers per two electrons) and a Faradaic efficiency of ca. 62 % (see SI section 4.3). In the absence of applied potential (OCP, open circuit potential), no ethyl acetate was formed (see SI, section 4.4). Likewise, in the absence of catalyst, the passed charge was significantly lower (7 C vs 40 C) with no detected formation of ethyl acetate. The observed catalytic activity compares well in terms of TON and product selectivity with other molecular homogeneous TH systems, with most systems being limited to the two-electron oxidation of secondary or benzylic alcohols. The Waymouth group reported a NNC ruthenium pincer for the oxidation of isopropanol to acetone with a TON of 4.[18] The same group reported on the usage of phenoxy mediators with an iridium pincer complex, reaching a TON of 8 for the same reaction.[21] Bonitatibus and co-workers demonstrated the activity of an iridium-based systems with a TON of 32 for the formation of *p*-benzaldehyde.[17] Appel and co-workers reported on a nickel (TON = 3.1)[15] and a cobalt triphos systems (TON = 19.9)[16] for benzaldehyde formation from benzyl alcohol. To the best of our knowledge, there is only one acceptor-less alcohol dehydrogenation (AAD) catalyst that has been activated electrochemically so-far,[23] generating acetone with a TON < 2. Only a handful of molecular systems are known to catalyze the electrochemical four electron alcohol reformation to esters, however at significantly higher potentials (1.15 V *vs* Fc^+/Fc^0). [2,26,27]

To achieve the transposition from thermal to electrochemical TH, both Grützmacher *et al.* and Waymouth took advantage of a fast equilibrium between the alcohol substrate and a metal hydride intermediate that could be readily oxidized. The chemistry of ruthenium pincer AAD systems is well studied (Scheme 1A) [24,28–32] and allows for a putative assignment of the observed CV-behavior. In the presence of excess base and alcohol (Figures 2 and 3), **1** is expected to yield dearomatized complex **2**,[24] as well as the alkoxide species **3**[24,31]. We might therefore assign the first wave at -0.5 V to the oxidation of dearomatized complex **2** and the wave around 0 V to the oxidation of the alkoxide complex **3**. Indeed, independently synthesized samples of **2** and **3** give rise to oxidation half-waves at -0.45 V and -0.1 V respectively (see SI, section 3 and 5.2). This is also in agreement with the observed behavior upon increasing the alcohol concentration with the expected consumption of dearomatized species **2** and concomitant disappearance of the first oxidation wave at -0.5 V. The equilibrium between **2**, **3** and **4** has been reported[31] and addition of excess ethanol to **2** is thus not only generating **3**, but also is expected to deliver **4** (Scheme 1A). The appearance of a new anodic wave at ca. -0.25 V (Figure 2) is thus attributed to the increasing formation of **4** upon addition of larger amounts of EtOH. Complex **4** is relatively unstable in solution,[24,31,32] and quickly reacts in the presence of supporting electrolyte to a new mono-hydric species **9** with a CV-response similar to **1** (see SI, section 3.2). Due to the instability of **4**, we used DFT calculations to predict its oxidation potential (see SI, section 6), which was in reasonable agreement with the observed wave (-0.19 V). The DFT calculations also confirmed the assignment of the other waves related to the dearomatized complex **2** (-0.33 V) and the ethoxide species **3** (-0.1 V).

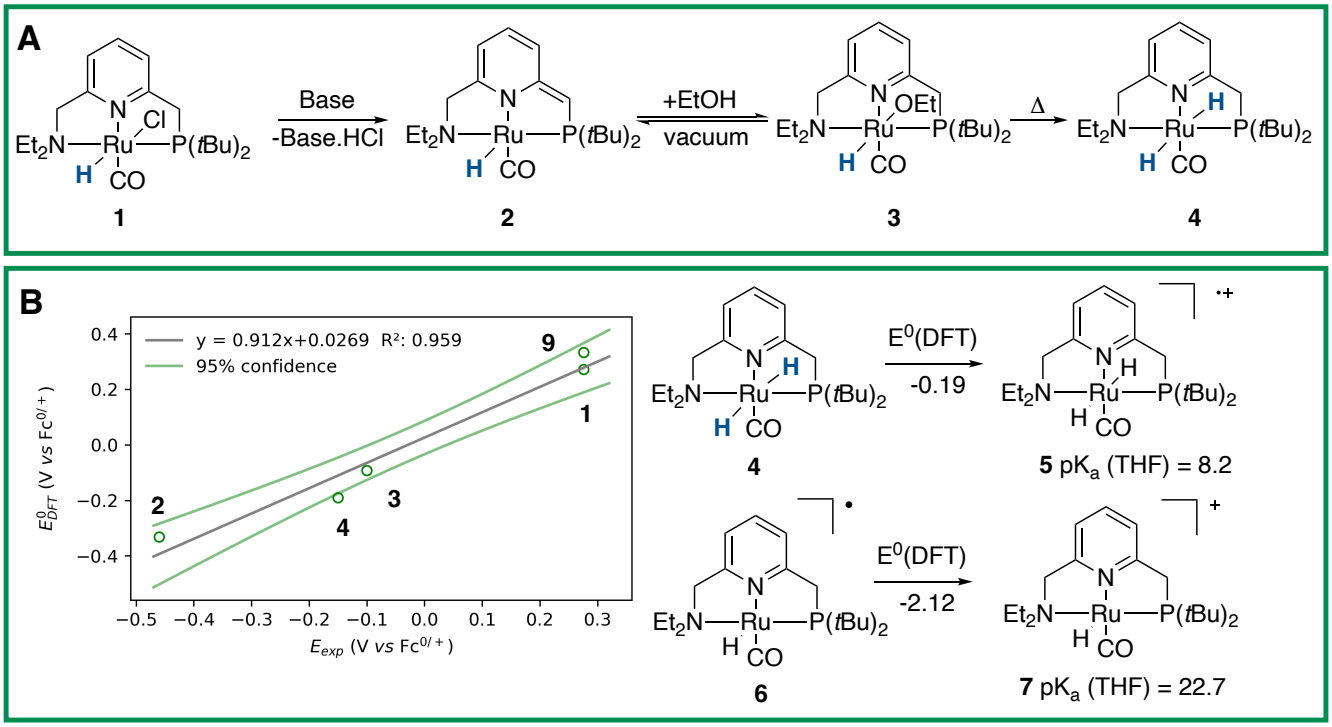

Scheme 1. A: Reactivity of pyridine-based ruthenium complexes *via* dearomatization/aromatization. B: Calculated standard potentials versus experimental oxidation potentials (see SI for details), as well as acidities of possible reactive intermediates.

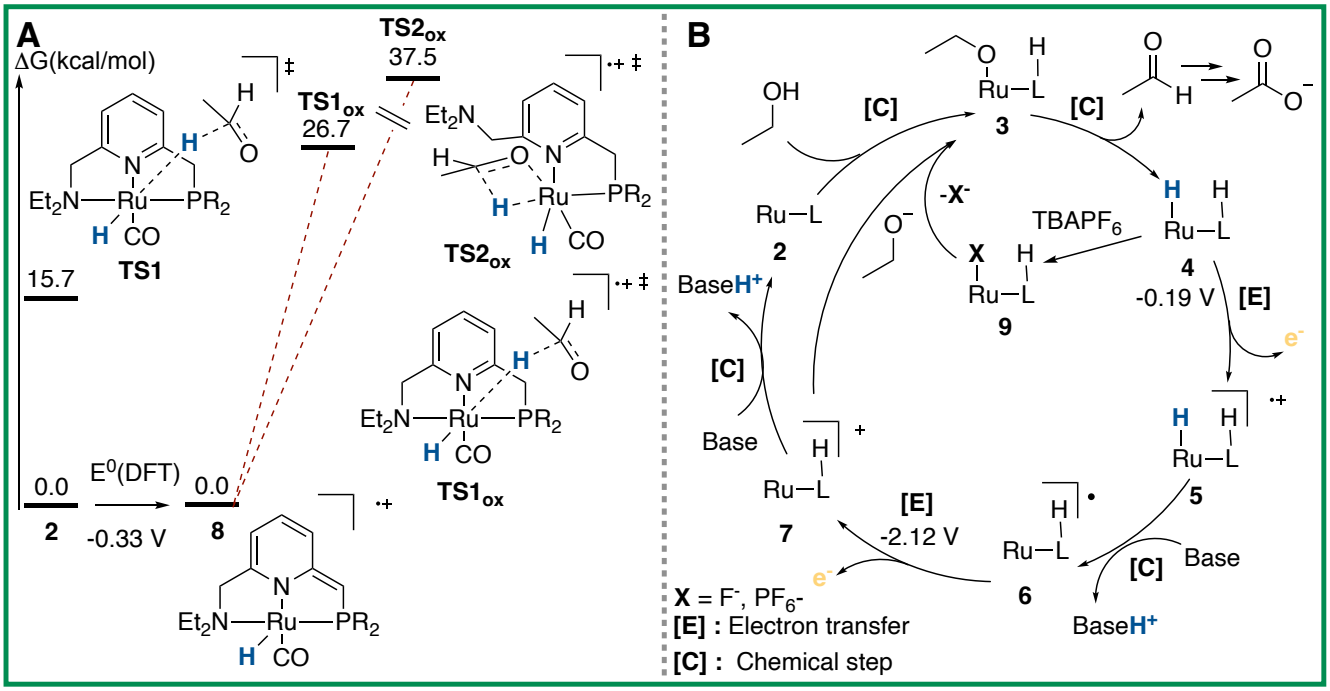

Scheme 2. Influence of oxidation on the dihydride transition states' energies. B: Possible catalytic cycle for the electrochemical alcohol oxidation promoted by **1**.

A more detailed mechanistic analysis remains currently hampered by the chemical instability of **4** under the employed reaction conditions. DFT calculations were thus used to get a better view on possible reaction pathways (Scheme 2B). The oxidation of **4** at -0.19 V (DFT) yields the radical cation **5**, with a calculated pK$_a$ in THF of 8.2 (see SI, section 6.3). In the presence of NaOEt, **5** should thus deprotonate readily to give radical **6**, which has an extremely negative oxidation potential of -2.1 V. At the potential it is generated, **6** should thus directly be oxidized to cationic complex **7**. This cationic species **7** has a

calculated pK_a of 22.7 in THF, which is in good agreement with experimental data from the Saouma group on a similar system.[25] The high pK_a of **7** in THF also validates the need for a strong base (e.g. NaOEt) to reform dearomatized **2**. Both Grützmacher and co-workers,[14] as well as Waymouth[23] have noted that the accelerating effect during electrocatalysis stems from the oxidation of a metal hydride intermediate that is generated by fast chemical steps. In order to verify this hypothesis and to exclude an electrochemical activation of this hydride formation step, transition state barriers were computed. Taking the dearomatized complex **2** as a reference point, generation of the dihydride **4** via a linear, charge-separated transition state **TS1** is associated with a barrier of 15.7 kcal/mol (Scheme 2A). The role of such linear transition states was highlighted recently in the case of ruthenium pincer catalysis for alcohol oxidation.[33–35] In principle, it might be envisioned that the oxidation of the metal center could be an additional driving force for this hydride abstraction step. However, after oxidation, the barrier rises by about 11 kcal/mol ($\mathbf{TS1_{ox}}$ = 26.7 kcal/mol, Scheme 2A). Likewise, a beta-hydride elimination *via* side-arm opening is not accelerated either by oxidation ($\mathbf{TS2_{ox}}$ = 37.5 kcal/mol). It thus seems that the generation of **4** is not accelerated by electron transfer steps and relies on a thermally activated chemical step. We can thus draw a possible catalytic cycle (Scheme 2B). Starting from dearomatized **2** or the alkoxide species **3** in the presence of a base and ethanol, a thermal chemical step delivers dihydride **4**. Complex **4** is oxidized at -0.19 V to the cation radical **5**, with a relatively low pK_a (8.2). Hence, fast deprotonation and reoxidation to the cation **7** follows. In the presence of base, **7** can then either undergo deprotonation to **2** or directly react with an alkoxide species to give **3** and close the catalytic cycle. The mono-hydride species **9**, also shows catalytic activity in the presence of substrate and base (see SI, section 3.1), which can be rationalized by the possible regeneration of **3** in the presence of alkoxides.

Conclusions

In conclusion, a Milstein-type catalyst (**1**) was activated electrochemically for the dehydrogenation of a primary alcohol to the corresponding ester. CV and DFT studies were used to propose a putative catalytic cycle, based on the chemical generation of dihydride intermediate **4** and its electrochemical conversion. It was shown that **1** can be used under preparative conditions yielding the four-electron oxidation products ethyl acetate and acetate, thus confirming successful electrification. We are currently exploring the electrochemical activation to other AAD systems and substrates, as well as to investigate the mechanism in more details. This will hopefully allow to address adverse deactivation pathways, as well as to design more active catalysts.

Data availability

All computed structures, including energies and thermochemistry is available free of charge via the ioChem-BD online repository under the following link: https://doi.org/10.19061/iochem-bd-6-117

Author Contributions

Conceptualization: N. v. W. data curation: N. v. W., D. T. electrochemistry: N. v. W., D. T. chemical synthesis: N. v. W., D. T. product analysis. N. v. W., D. T., E. N. DFT calculations: N. v. W. funding acquisition: N. v. W. writing original draft; N. v. W. reviewing: N. v. W., M. R., D. M.

Conflicts of interest

There are no conflicts to declare.

Acknowledgements

NvW is thankful for funding from the IdEx Université de Paris 2019, ANR-18-IDEX-0001. Computations were performed using HPC resources from GENCI-CINES (Grant 2019AP010811227).

ORCID

Niklas von Wolff: 0000-0001-8108-5365
Damien Tocqueville: 0000-0002-5169-436X
Marc Robert: 0000-0001-7042-4106
David Milstein: 0000-0002-2320-0262

Notes and references

1 The Future of Petrochemicals – Analysis, https://www.iea.org/reports/the-future-of-petrochemicals, (accessed October 26, 2021).
2 N. von Wolff, O. Rivada-Wheelaghan and D. Tocqueville, *ChemElectroChem*, , DOI:10.1002/celc.202100617.
3 M. Bellini, M. Bevilacqua, A. Marchionni, H. A. Miller, J. Filippi, H. Grützmacher and F. Vizza, *European Journal of Inorganic Chemistry*, 2018, **2018**, 4393–4412.
4 A. W. Cook and K. M. Waldie, *ACS Appl. Energy Mater.*, 2020, **3**, 38–46.
5 Y. Holade, K. Servat, S. Tingry, T. W. Napporn, H. Remita, D. Cornu and K. B. Kokoh, *ChemPhysChem*, 2017, **18**, 2573–2605.
6 J. Chen, S. Lv and S. Tian, *ChemSusChem*, 2019, **12**, 115–132.
7 F. Wang and S. S. Stahl, *Acc. Chem. Res.*, 2020, **53**, 561–574.
8 A. Badalyan and S. S. Stahl, *Nature*, 2016, **535**, 406.
9 J. E. Nutting, M. Rafiee and S. S. Stahl, *Chem. Rev.*, 2018, **118**, 4834–4885.
10 M. Rafiee, M. Alherech, S. D. Karlen and S. S. Stahl, *J. Am. Chem. Soc.*, 2019, **141**, 15266–15276.
11 M. Rafiee, Z. M. Konz, M. D. Graaf, H. F. Koolman and S. S. Stahl, *ACS Catal.*, 2018, **8**, 6738–6744.
12 A. C. Cardiel, B. J. Taitt and K.-S. Choi, *ACS Sustainable Chem. Eng.*, 2019, **7**, 11138–11149.
13 B. J. Taitt, M. T. Bender and K.-S. Choi, *ACS Catal.*, 2020, **10**, 265–275.

14 S. P. Annen, V. Bambagioni, M. Bevilacqua, J. Filippi, A. Marchionni, W. Oberhauser, H. Schönberg, F. Vizza, C. Bianchini and H. Grützmacher, *Angewandte Chemie International Edition*, 2010, **49**, 7229–7233.
15 C. J. Weiss, E. S. Wiedner, J. A. S. Roberts and A. M. Appel, *Chem. Commun.*, 2015, **51**, 6172–6174.
16 S. P. Heins, P. E. Schneider, A. L. Speelman, S. Hammes-Schiffer and A. M. Appel, *ACS Catal.*, 2021, **11**, 6384–6389.
17 P. J. Bonitatibus, M. P. Rainka, A. J. Peters, D. L. Simone and M. D. Doherty, *Chem. Commun.*, 2013, **49**, 10581–10583.
18 E. A. McLoughlin, K. C. Armstrong and R. M. Waymouth, *ACS Catal.*, 2020, **10**, 11654–11662.
19 K. R. Brownell, C. C. L. McCrory, C. E. D. Chidsey, R. H. Perry, R. N. Zare and R. M. Waymouth, *J. Am. Chem. Soc.*, 2013, **135**, 14299–14305.
20 M. Buonaiuto, A. G. De Crisci, T. F. Jaramillo and R. M. Waymouth, *ACS Catal.*, 2015, **5**, 7343–7349.
21 C. M. Galvin and R. M. Waymouth, *J. Am. Chem. Soc.*, 2020, **142**, 19368–19378.
22 M. Trincado, J. Bösken and H. Grützmacher, *Coordination Chemistry Reviews*, 2021, **443**, 213967.
23 E. A. McLoughlin, B. D. Matson, R. Sarangi and R. M. Waymouth, *Inorg. Chem.*, 2020, **59**, 1453–1460.
24 J. Zhang, G. Leitus, Y. Ben-David and D. Milstein, *J. Am. Chem. Soc.*, 2005, **127**, 10840–10841.
25 C. L. Mathis, J. Geary, Y. Ardon, M. S. Reese, M. A. Philliber, R. T. VanderLinden and C. T. Saouma, *J. Am. Chem. Soc.*, 2019, **141**, 14317–14328.
26 G. J. Matare, M. E. Tess, Y. Yang, K. A. Abboud and L. McElwee-White, *Organometallics*, 2002, **21**, 711–716.
27 M. E. Tess, P. L. Hill, K. E. Torraca, M. E. Kerr, K. A. Abboud and L. McElwee-White, *Inorg. Chem.*, 2000, **39**, 3942–3944.
28 C. Gunanathan, Y. Ben-David and D. Milstein, *Science*, 2007, **317**, 790.
29 J. R. Khusnutdinova and D. Milstein, *Angewandte Chemie International Edition*, 2015, **54**, 12236–12273.
30 T. He, J. C. Buttner, E. F. Reynolds, J. Pham, J. C. Malek, J. M. Keith and A. R. Chianese, *J. Am. Chem. Soc.*, 2019, **141**, 17404–17413.
31 D. G. Gusev, *Organometallics*, 2020, **39**, 258–270.
32 J. Zhang, G. Leitus, Y. Ben-David and D. Milstein, *Angewandte Chemie International Edition*, 2006, **45**, 1113–1115.
33 N. Govindarajan, V. Sinha, M. Trincado, H. Grützmacher, E. J. Meijer and B. de Bruin, , DOI:10.26434/chemrxiv.8947427.v1.
34 V. Sinha, N. Govindarajan, B. de Bruin and E. J. Meijer, *ACS Catal.*, 2018, **8**, 6908–6913.
35 Y.-Q. Zou, N. von Wolff, M. Rauch, M. Feller, Q.-Q. Zhou, A. Anaby, Y. Diskin-Posner, L. J. W. Shimon, L. Avram, Y. Ben-David and D. Milstein, *Chemistry – A European Journal*, 2021, **27**, 4715–4722.